Proceedings of the ICBBG2025
2025 International conference on Bio-mediated and Bio-inspired Geotechnics
18-20 May, 2025 | Tempe, Arizona, USA
https://doi.org/10.53243/ICBBG2025-103

Laboratory Evaluation of Vertical Burrowing Behavior of a Bioinspired Robot (BurroBot)

Sarina Shahhosseini[1] and Junliang (Julian) Tao[2*]

[1]Graduate Research Associate, School of Sustainable Engineering and the Built Environment, Center for Bio-mediated and Bio-inspired Geotechnics, Arizona State University, 650 E Tyler Mall, Tempe, AZ, 85281; Email: sshahho1@asu.edu
[2*]Associate Professor, School of Sustainable Engineering and the Built Environment, Center for Bio-mediated and Bio-inspired Geotechnics, Arizona State University, 650 E Tyler Mall, Tempe, AZ, 85281; Email: jtao25@asu.edu ; Corresponding author

ABSTRACT

Burrowing robots hold significant promise for applications in exploration, search-and-rescue, underground sensor deployment, and construction. However, they face challenges due to high soil resistance and complex soil-robot interactions that are less understood compared to movement in air or water. Drawing inspiration from biological organisms that efficiently navigate through soil, we propose a novel BurroBot, integrating reciprocating (dual-anchor) and helical mechanisms to achieve downward burrowing. The BurroBot features top and bottom augers connected by a two-segment stator and operates in dual-anchor mode, relying on alternate auger rotation and linear motion to overcome soil resistance. Prototyped using rapid manufacturing techniques and tested in loose-packed granular media (poppy seeds), the robot successfully demonstrated downward burrowing starting at different embedment depths. Results showed that while the robot could burrow down through the medium, the rate of advancement decreased with depth, and there was significant variability between trials due to changes in soil states. In each trial, burrowing stopped due to ceased auger rotations due to motor torque limitations. These findings highlight the complexities of soil-structure interactions in robotic burrowing and suggest that further optimization in robot design and control, as well as improved sample preparation methods, are necessary to enhance burrowing efficiency and repeatability.

Keywords: burrowing, robot, bio-inspired, helical, dual-anchor

INTRODUCTION

Burrowing robots are a new type of mobile robots designed to move through soil for tasks like exploration, search-and-rescue, sensor deployment, inspection, monitoring, transport, and construction (Tao 2021). Unlike moving in water, air, or on solid surfaces, burrowing in soil is less studied and understood. To burrow, robots must overcome soil resistance and surface friction, which are much higher than in air or water. Additionally, soil has vertical stress and strength gradients, requiring more force to burrow deeper. When burrowing horizontally, the presence of soil gradients and the free surface create a net upward lift force on a symmetric burrowing object, causing it to tilt towards the surface. As the robot moves, it also changes the soil structure, adding complexity to the task. All these factors make

burrowing and steering in the soil a challenge.

Despite its complexity and difficulty, moving in soil is common in nature and is often vital for the survival of soil inhabitants. Living organisms move in soil by changing their body shapes and often exploiting the solid-fluid phase transition of soil (Dorgan 2015; Hosoi and Goldman 2015). Many biological burrowing mechanisms have been identified and emulated, including dual-anchor by razor clams (Tao et al. 2020; Winter et al. 2014), Fig. 1 (a)-(b), and earthworms (Dorgan 2015). To facilitate burrowing, seed awns and worm lizards rely on rotation to reduce drag forces (Fig. 1 (c)-(d)). Drawing inspirations from these biological burrowing strategies, we have designed soft and rigid robots for upward and horizontal burrowing (Fig. 2 (a)-(c)).

Burrowing in sand is also analogous to swimming in low-Reynolds number viscous fluid, where the media-structure interaction resistance dominates over the inertial effects. Of particular interests in this research is spiral-shaped spirillum bacteria, which depend on a morphological helical cell as a survival tool to diffuse in viscous environments Fig. 1 (e) (Young 2006). The rotation of the helical cell breaks the time-reversal symmetry and generates a net propulsive force needed for its translational "swimming" movement (Cohen and Boyle 2010; DiLuzio et al. 2005; Qiu et al. 2014). Similarly, the Sandfish lizard's undulatory body movement results in a sinusoidal trace; this motion can be conceptualized as a two-dimensional analog to three-dimensional helical rotation (Fig. 1 (f)) (Maladen et al. 2011). All these inspirations hint at a helically-driven burrowing robot, which we preliminarily explored recently (Fig. 2 (d)-(e)). More recently, we adopted a coupled Discrete Element Method and Multi-body Dynamic approach to simulate a dual-auger robot's penetration in dry granular media (Shahhosseini et al. 2023; Shahhosseini and Tao 2025).

In this paper, we propose a new robot design that integrate the reciprocating (dual-anchor) and helical mechanisms and report its burrowing behavior in preliminary tests.

METHODOLOGY

Design of the Burrowing Robot: Body and Burrowing Mechanisms.

The design consists of three main components: a top auger, a bottom auger, and a two-segment stator (upper and lower stators) between them (Fig. 3). Both augers share the same handedness and are driven by separate gear motors. Their rotation reduces drag by decreasing the particle-penetrator contact number, the magnitude of contact forces, while redirecting these contact forces further away from the penetration axis (Tang and Tao 2022). Because the auger blades are asymmetrical, their rotation also produces a net thrust along the penetration direction (Bagheri et al. 2023).

A linear actuator connects the upper and lower stators, enabling reciprocating motion between them. Its off-center placement increases the stators' resistance to rotation and thus provides counter-torque to the augers, preventing the stators from rotating excessively.

The robot can operate in two burrowing modes: continuous-rotation and dual-anchor modes. In continuous-rotation mode, the linear actuator remains retracted, and both augers rotate in the same direction. In dual-anchor mode (Fig. 3 (d)), the augers rotate alternately in coordination with the linear actuator's extension and contraction (Shahhosseini and Tao 2025). During contraction phase, the top auger rotates to reduce resistance while the bottom auger anchors; the downward displacement of the top auger is termed "advancement". During extension phase, the bottom auger rotates to break the soil and reduce penetration resistance

while the top auger acts as an anchor.

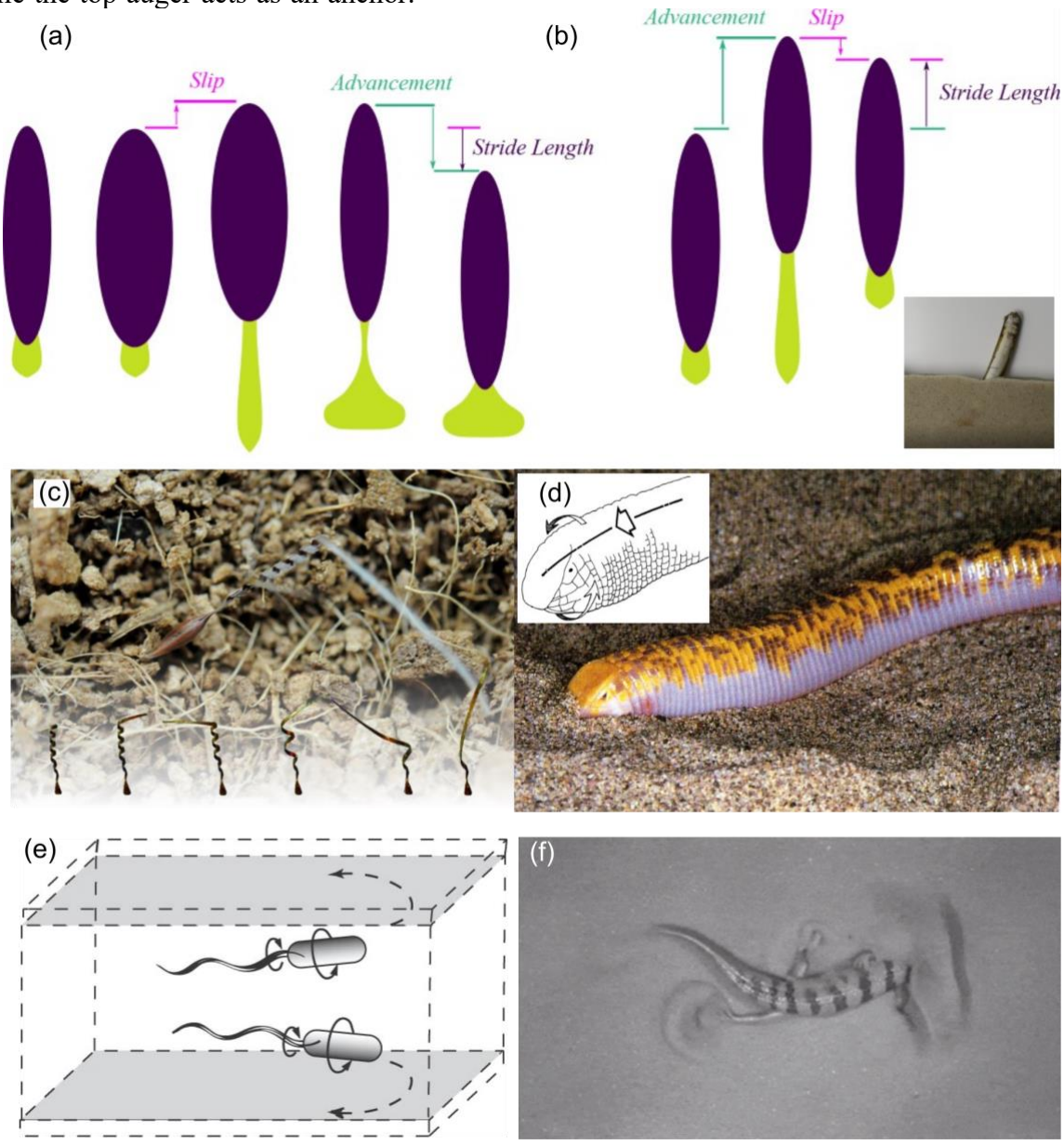

Fig. 1. Biological models and the proposed horizontal burrowing mechanism: (a) downward burrowing strategy for razor clam (Tao et al. 2020); (b) upward burrowing strategy for razor clam (Tao et al. 2020) and the inset shows a burrowing razor clam (*Ensis directus*); (c) Seed of *Pelargonium carnosum* digging into the ground by unwinding its awn (Jung et al. 2014); (d) angled worm lizards *Agamodon angeliceps*, (Cogger et al. 1998) and the inset illustrates its oscillatory motion during burrowing, adapted from (Gans 1974); (e) *E. coli* swims like a corkscrew (DiLuzio et al. 2005); (f) Sandfish *Scincus scincus* burrows into soil (Maladen et al. 2011).

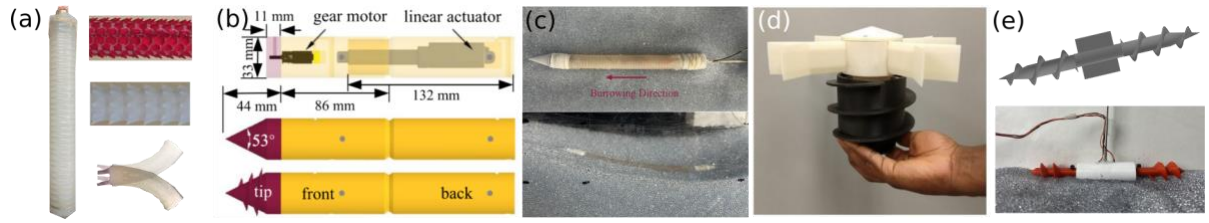

Fig. 2. Previous robots designed by the research team. (a) Soft upward burrowing robots (Huang et al. 2020; Tao et al. 2020); (b) Reciprocating horizontal burrowing robots with rotating tips (Zhong et al. 2023); (c) Soft horizontal burrowing robot with rotating tips (Tang et al. 2024); (d) Helical downward burrowing robot (Bagheri et al. 2023); (e) Helical horizontal burrowing robot (Shahhosseini et al. 2023).

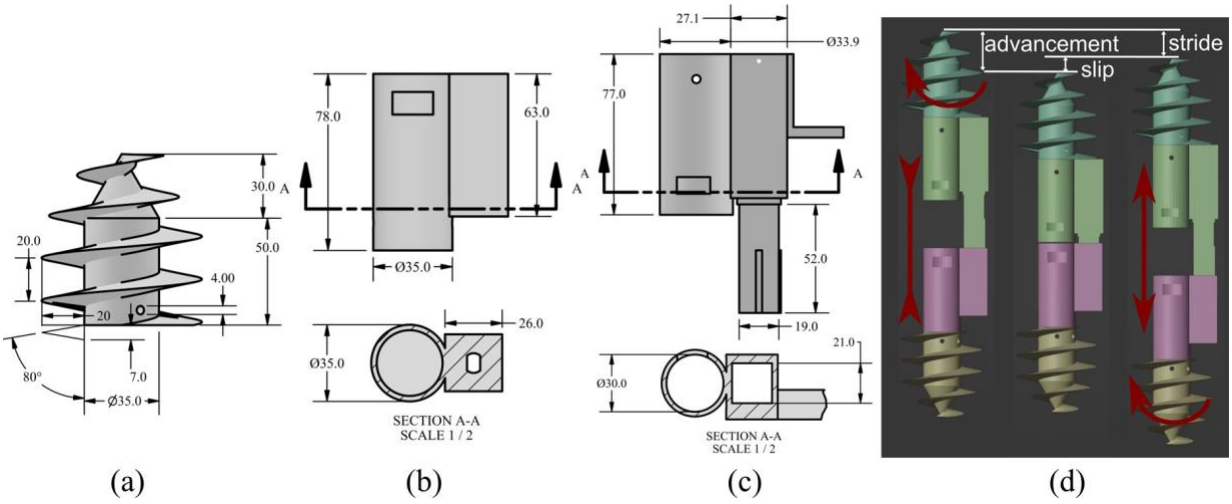

Fig. 3. Detailed dimensions of the robot's components. (a) Augers; (b) Upper stator; (c) Lower stator; (d) Assembled view and illustration of the dual-anchor mode burrowing. All dimensions are in cm.

When the anchors are less effective, "slip" can occur, reducing the overall "stride" length (Fig. 3 (d)). It is hypothesized that the continuous-rotation mode is more effective for horizontal or shallow downward burrowing, whereas the dual-anchor modes is better suited for deep burrowing, where pure rotation alone cannot generate enough thrust to overcome the increased resistance. In this paper, only the dual-anchor mode is tested.

Prototyping.

The robot was fabricated using rapid prototyping methods. The exterior was 3D printed with PLA, and the robot was powered by off-the-shelf components: Pololu 4846 gear motors (25Dx69L mm HP 12V with 48 CPR Encoder) and a miniature Actuonix linear actuator (#L12-50-100-12-P) which gives a maximum extension of 3 cm. A finished view of the robot in its extended and contracted states is shown in Fig. 4 (a).

The control system, illustrated in Fig. 4 (b), consists of an Arduino Uno and motor drivers (Pololu#2517). The auger rotation speeds were managed using PWM signals and a PID controller, both implemented in the Arduino.

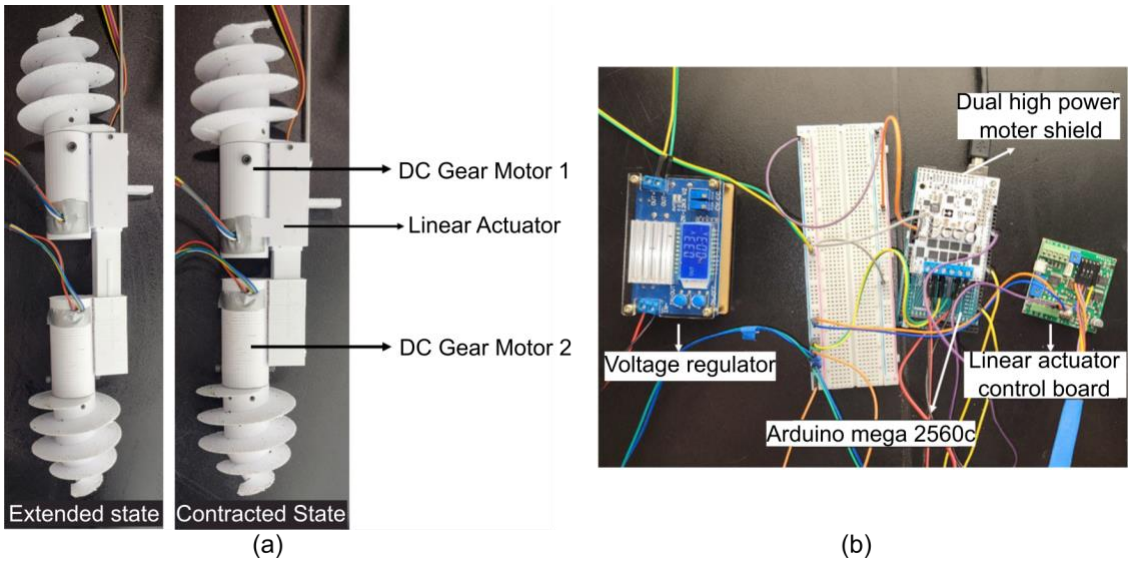

Fig. 4. Rapid Prototyping (a) Assembled of the 3D printed BurroBot (b) Control Circuit.

Experimental Testing.

For this experiment, an 80 cm tall container with a 30 cm diameter circular base was used. Poppy seeds, with rounded, kidney-shaped particles and a D_{50} of 0.7 mm were used due to their relatively low specific gravity (~0.65). Poppy seeds were poured layer by layer from a height of 1 cm to ensure uniform loose packing with an average relative density of about 35%. After reaching the desired fill height, the robot was placed at the center of the container, and additional poppy seeds were added to achieve the target embedment depth. Two embedment depths, 7 cm and 4 cm, were tested, with each experiment repeated three times.

At the start of each trial, the robot was fully extended, and the augers rotated at a constant speed of 50 RPM when activated alternately. The extension and contraction of linear actuator lasts for 2.5 s each with a speed of 1 cm/s. Therefore, the period of each cycle is 5 s.

A stainless-steel rod was attached to the linear actuator box for measurement purposes, with visible markers placed along the rod to track its movement (Fig. 5). The actuator's motion was recorded using a video camera, and the data were analyzed using an optical-flow algorithm implemented in Python with a computer vision package opencv-python (OpenCV Community 2023). This algorithm tracked the displacement of the markers frame by frame, enabling precise measurement of the actuator's movement. Fig. 5 shows the first and last frames of the video recorded during the downward burrowing test with an initial embedment depth of 7 cm.

RESULTS

Burrowing behavior.

The relative burrowing displacements of the robot for each trial is shown in Fig. 6. Each trial of the dual-anchor mode was successful as the robot gradually burrowed downward, albeit at a slow pace. However, the burrowing curves showed significant variation between trials with the same initial embedment depth.

In all trials, during each cycle, the robot advanced downward during the contraction

phase, and slipped upward during the extension phase. The difference between the downward advancement and upward slip led to the robot's overall stride. On average, the robot achieved a self-burrowing depth of 2.5 cm in under two minutes.

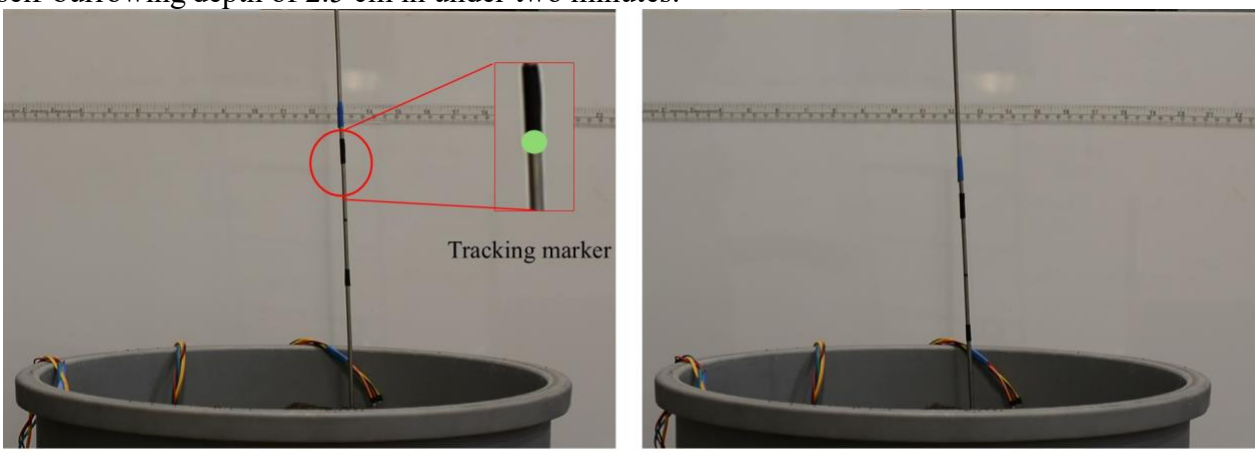

Fig. 5. Snapshot of the burrowing process which lasted for 150 seconds. (a) t = 0s; (b) t = 150s.

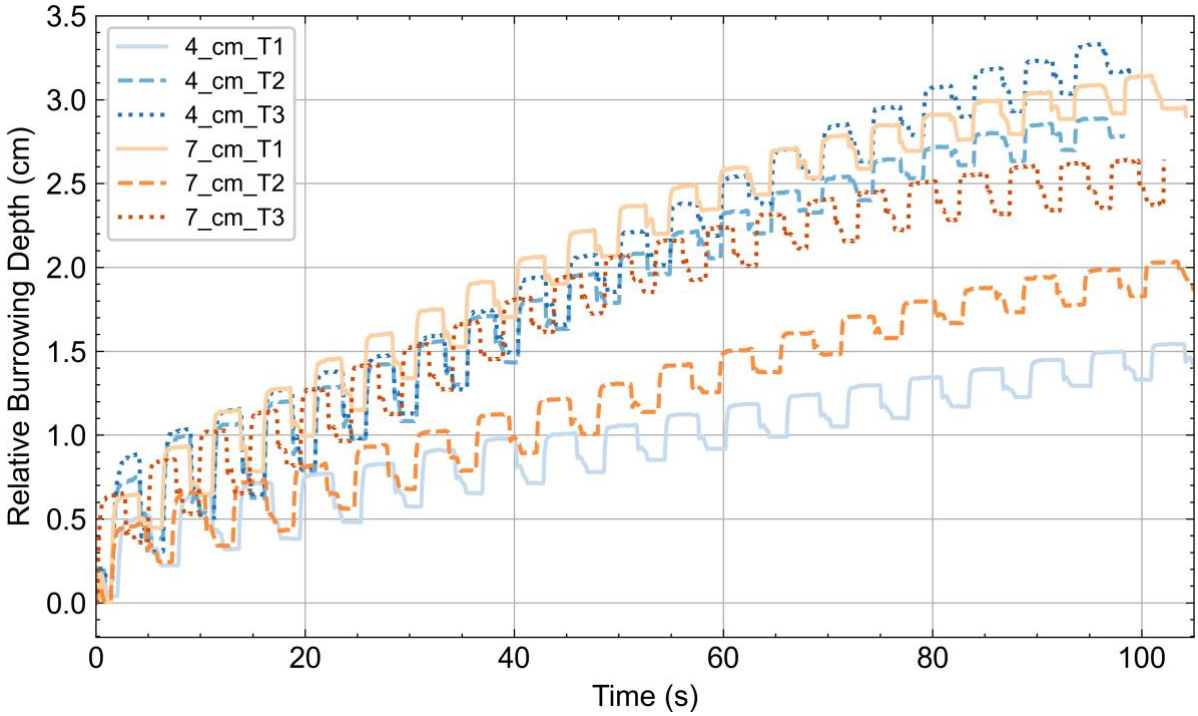

Fig. 6. Burrowing curves for all trials.

Fig. 7 summarizes the trends of the characteristic lengths including the advancement, slip and stride length. All characteristic lengths exhibited a decreasing trend with increasing cycle number or depth, with the rate of decrease being highest for advancement.

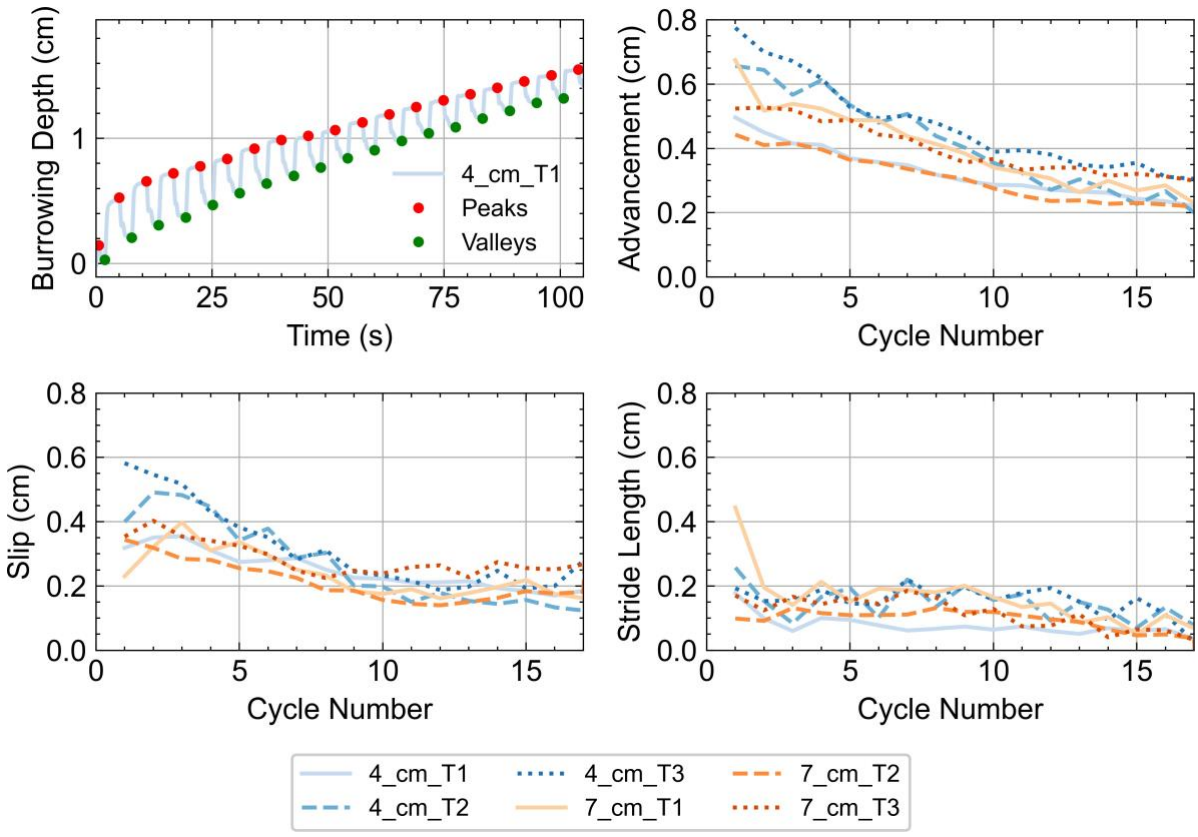

Fig. 7. Advancement, slip and stride lengths over time for all the trials. (a) Illustration of the identified peak and valley points; (b) Advancement trends; (c) Slip trends; (d) Stride length trends.

The rapid decline in advancement during the contraction phase is not easily explained. We initially expected that advancement would increase with depth, assuming constant auger rotation and linear actuator speeds, since a deeper robot should theoretically benefit from a more effective bottom anchor. However, as depth increases, the pulling (or resistance) force on the top auger during the contraction phase may also intensify. The amount of advancement is not determined solely by the ultimate anchoring force of the bottom auger or the penetration resistance of the top auger, but by the mobilization of these forces during displacement, which is influenced by the stiffness of the surrounding soil. Greater advancements occur when the bottom auger's anchoring force mobilizes more quickly, while the top auger's penetration resistance mobilizes more gradually, and vice versa.

In each trial, slip decreased with depth because the top anchor became more effective as the robot moved further from the free surface. As depth increases, the stress level rises and the failure mode around the top anchor transits from shallow to deep failure. Both factors contribute to an increase in anchoring strength.

Since the rate of decrease in advancement slightly outweighed the reduction in slip, the overall stride length was marginal but still exhibited a decreasing trend, indicating reduced burrowing effectiveness.

Encountered Challenges and Inconsistent Trends.
As the robot penetrated further, the bottom auger encountered rotation issues, likely due to the resistance torque exceeding the torque provided by the DC motor. In all trials, the experiment was halted when the bottom auger ceased rotation because of the increased torque from the surrounding particles. Additionally, even with the same initial embedment depth, the burrowing curves exhibited significant variation across trials. When averaged, there were no substantial differences between the two test cases with different initial embedment depths.

These observations suggest that the robot's behavior is highly dependent on the packing and stress state of the granular material. Downward burrowing likely causes densification and strengthening of the granular material ahead of the robot, leading to an increased torque requirement for rotation. If the soil state did not change due to burrowing, then after the robot burrowed an additional 3 cm from an initial embedment of 4 cm—reaching a depth of 7 cm—it should have repeated the burrowing process observed in the 7 cm initial embedment case. However, this did not occur; the auger ceased to rotate upon reaching 7 cm depth.
Furthermore, the initial sample state affects the burrowing behavior, as shown by the variations among trials with the same initial embedment depths. Although we exercised caution when preparing all the samples, the repeatability of the current sample preparation method is low and it is also too laborious. An automatic, repeatable method of sample preparation is highly desired and will be explored next.

CONCLUSIONS

In this study, we introduced a novel burrowing robot that integrates reciprocating (dual-anchor) and helical mechanisms, inspired by biological burrowing strategies. The robot was successfully prototyped and tested in granular media, demonstrating its ability to burrow downward in dual-anchor mode. However, the advancement decreased with depth, and significant variability was observed between trials with the same initial embedment depth. These trends are attributed to the increasing soil resistance at greater depths, torque limitations of the auger motors, and changes in the soil state caused by the burrowing process itself.

The challenges encountered highlight the complexities of soil-structure interactions in robotic burrowing. Future work will focus on enhancing the torque capabilities of the motors, optimizing the auger design to reduce resistance, and developing an automated, repeatable sample preparation method to improve experimental consistency. Additionally, exploring alternative operational modes and control strategies may help to mitigate the effects of soil densification and improve overall burrowing efficiency. By addressing these challenges, we aim to advance the design and functionality of burrowing robots, paving the way for practical applications in subterranean exploration, search-and-rescue operations, and underground construction.

ACKNOWLEDGEMENTS

This work is supported by the National Science Foundation (NSF) under awards CMMI 1849674 and CMMI 1841574, and by the Office of Naval Research (ONR) SBIR/STTR Program N24A-T017. Any opinions, findings, conclusions, or recommendations expressed in this material are those of the authors and do not necessarily reflect the views of the NSF or ONR.

REFERENCES

Bagheri, H., D. Stockwell, B. Bethke, N. K. Okwae, D. Aukes, J. Tao, and H. Marvi. 2023. "A bio-inspired helically driven self-burrowing robot." *Acta Geotech.* https://doi.org/10.1007/s11440-023-01882-9.

Cogger, H. G., R. G. Zweifel, and D. Kirshner. 1998. *Encyclopedia of reptiles & amphibians*. Weldon Owen.

Cohen, N., and J. H. Boyle. 2010. "Swimming at low reynolds number: A beginners guide to undulatory locomotion." *Contemporary Physics*, 51 (2): 103–123. https://doi.org/10.1080/00107510903268381.

DiLuzio, W. R., L. Turner, M. Mayer, P. Garstecki, D. B. Weibel, H. C. Berg, and G. M. Whitesides. 2005. "Escherichia coli swim on the right-hand side." *Nature*, 435 (7046): 1271–1274. https://doi.org/10.1038/nature03660.

Dorgan, K. M. 2015. "The biomechanics of burrowing and boring." *Journal of Experimental Biology*, 218 (2): 176–183. https://doi.org/10.1242/jeb.086983.

Gans, C. 1974. "Analysis by comparison: Burrowing in amphisbaenians." *Biomechanics: An Approach to Vertebrate Biology*, 117–191.

Hosoi, A. E., and D. I. Goldman. 2015. "Beneath our feet: Strategies for locomotion in granular media." *Annu. Rev. Fluid Mech.*, 47 (1): 431–453. https://doi.org/10.1146/annurev-fluid-010313-141324.

Huang, S., Y. Tang, H. Bagheri, D. Li, A. Ardente, D. Aukes, H. Marvi, and J. Tao. 2020. "Effects of friction anisotropy on upward burrowing behavior of soft robots in granular materials." *Advanced Intelligent Systems*, 2 (6): 1900183. https://doi.org/10.1002/aisy.201900183.

Jung, W., W. Kim, and H.-Y. Kim. 2014. "Self-burial mechanics of hygroscopically responsive awns." *Integrative and Comparative Biology*, 54 (6): 1034–1042. https://doi.org/10.1093/icb/icu026.

Maladen, R. D., Y. Ding, P. B. Umbanhowar, A. Kamor, and D. I. Goldman. 2011. "Mechanical models of sandfish locomotion reveal principles of high performance subsurface sand-swimming." *Journal of The Royal Society Interface*. https://doi.org/10.1098/rsif.2010.0678.

OpenCV Community. 2023. "OpenCV-Python." https://pypi.org/project/opencv-python/.

Qiu, T., T.-C. Lee, A. G. Mark, K. I. Morozov, R. Münster, O. Mierka, S. Turek, A. M. Leshansky, and P. Fischer. 2014. "Swimming by reciprocal motion at low reynolds number." *Nat Commun*, 5 (1): 5119. https://doi.org/10.1038/ncomms6119.

Shahhosseini, S., M. Parekh, and J. Tao. 2023. "DEM-MBD coupled simulation of a burrowing robot in dry sand." *Geo-congress 2023*, 309–317. Los Angeles, California: American Society of Civil Engineers.

Shahhosseini, S., and J. Tao. 2025. "Bio-inspired dual-auger vertical self-burrowing robot: DEM-MBD analysis of downward penetration in granular media." *GeoFrontiers 2025*.

Tang, Y., and J. Tao. 2022. "Multiscale analysis of rotational penetration in shallow dry sand and implications for self-burrowing robot design." *Acta Geotechnica*. https://doi.org/10.1007/s11440-022-01492-x.

Tang, Y., Y. Zhong, and J. Tao. 2024. "Bio-inspired rotational penetration and horizontal self-burrowing soft robot." *Acta Geotech.* https://doi.org/10.1007/s11440-023-02173-z.

Tao, J. 2021. "Burrowing soft robots break new ground." *Science Robotics*, 6 (55): eabj3615. https://doi.org/10.1126/scirobotics.abj3615.

Tao, J., S. Huang, and Y. Tang. 2020. "SBOR: A minimalistic soft self-burrowing-out robot inspired by razor clams." *Bioinspiration & Biomimetics*, 15 (5): 055003. https://doi.org/10.1088/1748-3190/ab8754.

Winter, A. G., V, R. L. H. Deits, A. H. Dorsch D. S. and Slocum, and A. E. Hosoi. 2014. "Razor clam to RoboClam: Burrowing drag reduction mechanisms and their robotic adaptation." *Bioinspir.*

Biomim., 9 (3): 036009. https://doi.org/10.1088/1748-3182/9/3/036009.

Young, K. D. 2006. "The selective value of bacterial shape." *Microbiol Mol Biol Rev*, 70 (3): 660–703. https://doi.org/10.1128/MMBR.00001-06.

Zhong, Y., S. Huang, and J. Tao. 2023. "Minimalistic horizontal burrowing robots." *Journal of Geotechnical and Geoenvironmental Engineering*, 149 (4): 02823001. https://doi.org/10.1061/JGGEFK.GTENG-11468